Proceedings of the 9th World Congress on Mechanical, Chemical, and Material Engineering (MCM'23)
Brunel University, London, United Kingdom –August 06-08, 2023
Paper No. HTFF 211
DOI: 10.11159/htff23.211

Effect of Forcing Amplitude during Lateral Sloshing At Low Liquid Depth

Sadham Usean Ramasamy*, Shyama Prasad Das, Shaligram Tiwari
Department of Mechanical Engineering, Indian Institute of Technology Madras
Chennai 600036, India
Email: sadhamramasamy@gmail.com

Abstract- In this study, experimental findings of heat and mass transfer across liquid-vapor interface in a partially filled cylindrical container of 100mm diameter with a maximum liquid (n-pentane) depth (h) of 30mm subjected to horizontal oscillations have been reported. In frequency range where the instability and wave breaking occur, as demonstrated in literature with waves in planar and chaotic regime, have been explored. The pressure drop caused by condensation is minimal when the liquid-vapor interface is at rest. Two different cases have been considered, viz. for chaotic regime with wave breaking at natural frequency (2.707 Hz) for non-dimensional amplitude (A/R) having values of 0.0022, 0.0026, and 0.0030 respectively. Similarly, the other case being for breaking wave with swirl (ω = 2.653 Hz and A/R values of 0.0084, 0.0088 and 0.0092 respectively). For both the cases, pressure and temperature decrease rapidly and significantly due to high condensation rate in presence of large amplitude sloshing. Pressure drops are found to be higher in breaking wave regime (ω = 2.653 Hz) where waves are chaotic. The temperature along the axis of the container at different instants are plotted and a significant drop in temperature in vapor whereas substantial rise in the liquid temperature is observed.

Keywords: Faraday waves, horizontal oscillation, cylindrical container (circular cross-section), single frequency excitation, asymmetric mode, sloshing.

Nomenclature

D	diameter of the teat container
R	radius of the test container
g	gravitational acceleration
S	liquid free surface
T	Temperature
h	height
P	pressure
ρ	density
ϑ	kinematic viscosity
T_s	saturation temperature
T_i	initial temperature
ω_f	forcing frequency
ω	wave frequency
K_{mn}	wave number
δ	damping ratio

δ_{m0} kronecker delta function

σ surface tension

A forcing amplitude

Subscripts

m nodal diameters

n nodal circles

i initial

f final

s saturation condition

1. Introduction

Liquid sloshing has wide range of engineering applications, including the aerospace industry, the design of fuel tanks for space vehicles and aircraft, the design of automotive fuel tanks, liquid transport containers on highways, ships, seismically excited storage tanks, dams, military vehicles, and nuclear reactors. Sloshing generates highly localized impact pressure on the walls, which can cause structural damage as well as enough moment to affect the stability of the vehicle transporting the liquid container. Fuel sloshing in an aircraft's drop tank or external auxiliary fuel storage tank can compromise the structural integrity of the drop tank and even cause it to fail completely. Sloshing within the tank is a serious problem in aerospace and automotive applications. Also large changes in pressure may occur in the fuel tanks of spacecraft as well as other liquefied gas storage tanks as a result of condensation or evaporation at the liquid-vapor interface due to sloshing.

When the tank is subjected to excitations in a way that causes the liquid-vapor interface to slosh, the pressure fluctuations and specifically the rate of pressure change, may get significantly increased. Understanding ways to connect the pressure change to the sloshing conditions is extremely important from both practical as well as theoretical standpoint. In a partially filled liquid hydrogen (LH2) tank that is pressurized to 250 kPa, Moran et al. [1] experimentally observed that a pressure shift (pressure drop) of around 100 kPa can happen in less than 10 s. As predicted, Arndt [2] reported that the presence of a non-condensable gas results in decreased rate of condensation and increased rate of evaporation. Following trials were restricted to sloshing conditions that were kept fixed. Parametrically forced waves, also referred to as Faraday waves that are sub-harmonically stimulated, were experimentally explored by Das and Hopfinger [3]. The stability and wave breaking boundaries for the mass transfer experiments in a partially filled cylindrical tank were investigated in their later experiments. They arrived to the conclusion that heat and mass transfers at the liquid-gas interface are greatly increased by large amplitude interfacial waves. In order to comprehend physical processes and the dependence of the pressure change on the physical qualities of the liquid and sloshing conditions, Das and Hopfinger [4] and Hopfinger and Das [5] experimentally studied volatile liquids that are storable at room temperature. They have created a condensation-evaporation model that accounts for the temperature gradient near the liquid-vapor interface, the rate of pressure change as a function of the liquid's physical characteristics (expressed by the Jakob number), and an effective thermal diffusivity that depends on the sloshing conditions. It was obvious that more tests and research were required to fully grasp the relationship between the pressure drop, temperature variation, and the sloshing conditions of liquids. Ludwig et al [6] studied the effects of planar, chaotic and swirl effect on the pressure drop in the cryogenic tank which is more realistic to the practical conditions in a propellant tank in launch vehicles and derived an expression for sloshing Nusselt number based on the sloshing Reynolds Number. Lacapere [7] studies mass transfer in LOX in a circular cylindrical tank and observed a large pressure drop and also simulated it numerically. The purpose of the present study is to perform experiments with non-cryogenic, volatile liquids under laboratory conditions in a controlled manner at various fluid depths and later attempts can be made to upscale results for other liquids.

The present study aims to understand the behaviour of fluid near the wall in terms of heat transfer due to sloshing effects at low liquid depths. To analyze the mass transfer across the liquid-vapor interface during sloshing due to the influence of the liquid levels on the free surface, the test facility is being created. The present research work focuses on the effect of forcing amplitude during lateral sloshing at low liquid depth. The asymmetric mode (1, 1) in a cylindrical container for low liquid depth of 30 mm. Two different cases have been considered, viz. at natural frequency (2.707 Hz) for forcing amplitudes

(A/R) having values 0.0022, 0.0026, and 0.0030 respectively. Similarly, the other cases being at ω = 2.653 Hz and A/R values of 0.0084, 0.0088 and 0.0092 respectively covering the chaotic regime of wave motion. We present the experimental results of the pressure drops as well as the temperature variations.

2. Experiments

The experiment setup has been shown in Fig.1. It includes the permanent magnetic Beckhoff Fp400N (AX5112 Driver) shaker, Wenglor CP24 laser displacement sensor, fixture arrangement, base plate, fuel tank, fuel supply line, fuel drain line, ball valve, thermocouple, electric heating plates, heat regulators, AC/DC amplifiers, drive, insulating material (glass wool), steel ruler, and computer with integrated software (TwinCAT). The horizontally oscillating permanent magnetic Beckhoff Fp400N (AX5112 Driver) shaker has a peak force of 440 N and holds a cylindrical transparent container partially made of acrylic, 100 mm in diameter and 120 mm in depth. The lower half of the container is made of acrylic material, allowing the interface to be visible to capture the interface and flow behaviour during oscillation.

The upper half of the container is made of aluminum with a 5 mm wall thickness for the mass transfer experiments. The base plate's bottom O-ring seal ensures that the two pieces are vacuum-tight after being screwed together. The thermocouples and pressure transducer locations at the top cover face are also in Fig. 1. The upper half of the aluminum component is wrapped in a heating wire to enable for temperature monitoring, and the upper half is also covered in aluminum foil and insulation to reduce heat gain from the outside. The wall temperature of upper part may be raised by around 20oC in 5 minutes from room temperature with the help of a heating power used. Conduction from the upper half through the wall causes the lower portion of the test cylinder to become somewhat heated. The experimental setup includes 17 thermocouples (probe type): 6 for the vapour section, 6 for the liquid section, 2 for the vapour generator (one for the vapour temperature and the other for the generator wall temperature), 2 for measuring the test section wall temperatures, 1 for measuring wall temperature of liquid tank, and 1 pressure transducer (Fig. 1). All thermocouples and the pressure transducer are connected to data acquisition (DAQ).

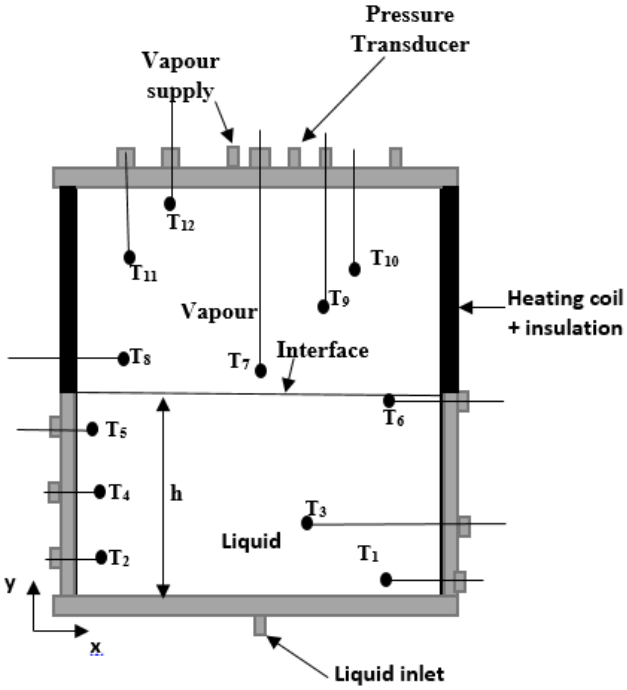

Fig.1. Schematic view of test rig. The thermocouples are numbered T_1 to T_{12}, located at height of 5, 10, 15, 20, 25, 30, 35, 40, 45, 50, 55, 60, and 65 mm

2.1 Evacuation, heating, and pressurization of the test rig

The test rig and vapour generator is evacuated using a vacuum pump, and the pressure of the vapour generator tank is about 3.5 bar. The test rig wall temperature is maintained at desired temperature (here, 55°C), by heating the coil wound around it with a power supply of 20 W. Majority of these investigations have been done in environments where condensation heat transfer takes place. The upper portion of the test cell, made of aluminum with total mass of 0.5 kg, is heated during the condensation experiments to the desired temperature. Liquid n-pentane from a degassed tank is supplied to the test rig after the desired temperature is achieved. The properties of n-pentane at 28oC are shown in Table 1. The pressure in the test ring is ramped up by infusing n-pentane vapour at a temperature much above the saturation temperature from the vapor generator. The pressure reaches approximately 3 bar in 30 seconds. Small disturbances are observed on the liquid surface owing to impingement and condensation during the infusion process. The pressure and temperature evolution during the filling process is shown in Fig. 2 and 3. Lateral sloshing experiments at the desired amplitude and frequency are started after a small wait at the end of pressurization. Experiments are conducted only in asymmetric (1, 1) mode. Two different types of experiments have been considered, viz. for stable wave motion at non-dimensional frequency (ω/ω_{11}) of 1 and non-dimensional amplitude (A/R) having values 0.0018, 0.0022, 0.0026, and 0.0030 respectively, with the forcing frequency (ω) of 2.707 Hz. Similarly, the other case being for breaking wave with ω/ω_{11}=0.98 and A/R values of 0.0084, 0.0088, 0.0092, and 0.0096 respectively, with ω = 2.653 Hz, are shown in Fig.4. Experiment1 conditions fall between the breaking and swirl wave regimes. Experiment2 conditions are in the chaotic wave regimes. As a result, the liquid movement happens more under experiment1 conditions than under experiment2. Additionally, compared to the planner regime, the swirl regime experiences higher variations in temperature and pressure.

Table 1: Properties of n-pentane

Fluid properties	
Temperature (°C)	28
Pressure (bar)	0.73168
Density (ρ) kg/m^3	618.95
Kinematic viscosity (ν) m^{2}s^{-1})	2.14E-04
Thermal conductivity (k) Wm^{-1}K^{-1}	0.11064
Surface tension (σ) Nm^{-1}	0.015261

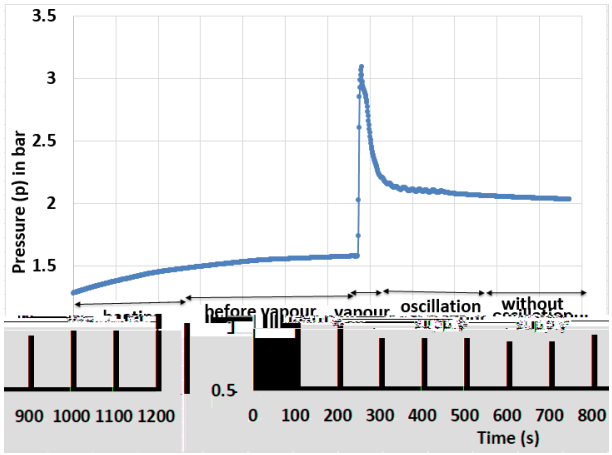

Fig.2. Pressure as a function of time (s) with sloshing (ω/ω_{11}=1; A/R = 0.0018)

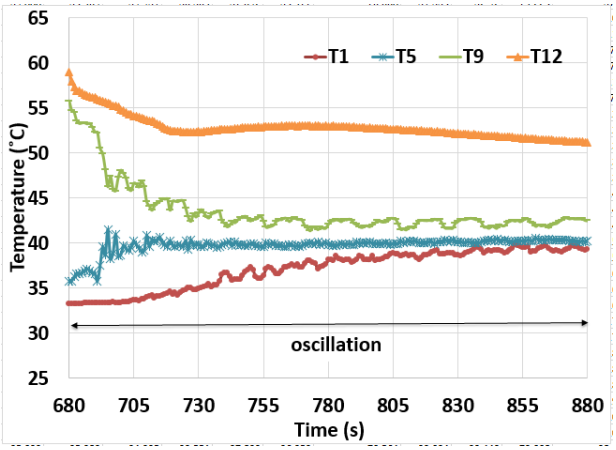

Fig.3. Temperature variations as a function of time (s) for thermocouples T1 and T5 (liquid region), and Thermocouples T9 and T12 (vapour region) during asymmetric oscillation for ω/ω_{11}=1; A/R = 0.0018

Temperature variation in the liquid during sloshing as a function of time is shown in Fig. 3. Experiments are conducted under the conditions ω/ω_{11}=1 and A/R = 0.0018, which is at breaking-swirl regimes. T5 thermocouple being at near a liquid-free surface, the temperature rises significantly during oscillation. The T1 thermocouple likewise increases, though less than the T5 thermocouple, which is located at larger liquid depth. Because the experiment1 conditions are all at swirl regimes, which have more liquid movement, the liquid has swirl motion along the clockwise direction during oscillation. In the same way, Fig. 3 displays the experimental findings of two vapour section thermocouples temperature values as a function of time. The values of the thermocouples T9 and T12 similarly rise during sloshing, but the thermocouple T5, which is situated extremely near the free surface, exhibits higher variation. Because it is situated quite close to the heater wall surface, the thermocouple T12 exhibits very little fluctuation. Because the swirl movement of the liquid hits and moves in a clockwise direction, the temperature fluctuations of the thermocouples significantly varies during the experiment1 condition.

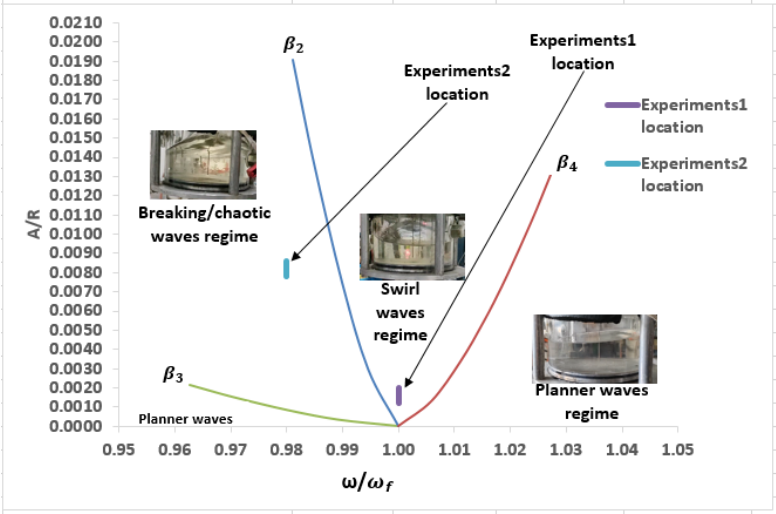

Fig.4. Phase diagram for dimensionless forcing amplitude (A/R) as a function of dimensionless frequency (ω/ω_f).

The vertical lines are the locations of experiments.

Phase diagram depicting the different regimes of the wave motion including the bifurcation lines is shown in Fig. 4. Equation (1) has been used to calculate the natural frequency ω/ω_{11} for the asymmetric sloshing (1, 1) mode. Similarly, the forcing frequency is calculated, which is used as the shaker's input frequency. After the vapour supply, the shaker must be turned on for 180 seconds to produce lateral sloshing about the x-axis. The upper heating system of the test rig is turned off as the sloshing process began. The natural frequency of wave mode can be obtained from the dispersion relation added with surface tension effects,

$$\omega_{mn}^2 = g k_{mn}\left(1 + \frac{{k_{mn}}^2 \sigma}{g\rho}\right) \tanh(k_{mn} \mathrm{d}) \tag{1}$$

where ω_{mn} is the natural frequency and the wave modes (m, n) express m nodal diameters and n − 1 +δ_{m0} nodal circles with m = 0, 1, . . . and n = 1, 2, . . ., where δ_{m0} is the Kronecker delta function. k_{mn}, g, σ, and ρ are the wave number, acceleration due to gravity, surface tension, and density of fluid.

$$\frac{A}{R} = \frac{1}{1.684}\left[\frac{\omega/\omega_f - 1}{\beta_i}\right]^{3/2} \tag{2}$$

where β is the difference between forcing frequency and natural frequency (frequency-offset parameter). Values of $\beta_2, \beta_3,$ and β_4 calculated from the experiments are -0.36, -1.55 and 0.7350, respectively. The solid lines in Fig.4 are the bifurcation lines obtained using Eq. (2). In both experiments, it was discovered that the wave motion was dependent on the forcing frequency, liquid depth, and forcing amplitude. When the forcing amplitude is high, the wave motion eventually becomes breaking/chaotic, swirl, and non-planar.

2.2 Pressure drop due to asymmetric lateral sloshing (asymmetric wave (1, 1) mode)

Variations in pressure with respect to time, a swirl wave motion at non-dimensional frequency ($\omega/\boldsymbol{\omega_{11}}$) of 1 and non-dimensional amplitude (A/R) having values 0.0018, 0.0022, and 0.0026 with the forcing frequency (ω) of 2.707 Hz are illustrated in Fig. 5. Also observed that the pressure drop increases during oscillation due to liquid swirling in a clockwise direction and decreases after oscillation. Further from that, swirl motion causes swirl-breaking regimes when the amplitude value increases and causes pressure values to fluctuate. Fig. 5 also clearly shows that at swirl regime, the pressure drop values develop as the amplitude (A/R) ratio increases. When compared to the curve without oscillation, the pressure drop is greater during oscillation. Also, experiments have been conducted without sloshing and compared with those under sloshing conditions as shown in Fig.5. The pressure loss for n-pentane in both swirl and breaking wave regimes has been reported. The rate of pressure drop for chaotic regime (breaking waves) is around an order of magnitude greater than the value for swirl regime.

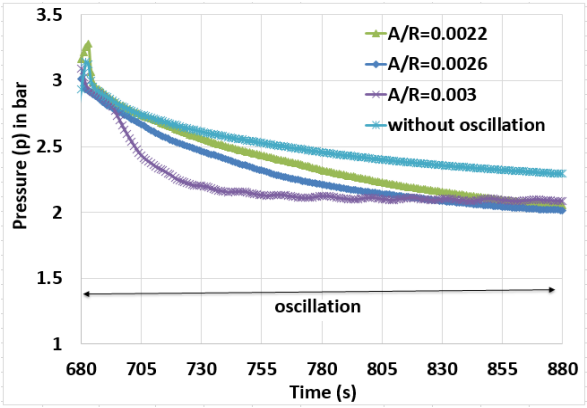

Fig.5. Pressure variations as a function of time (s) for swirl wave motion at non-dimensional frequency (ω/ω_{11}) of 1 and non-dimensional amplitude (A/R) of 0.0022, 0.0026, and 0.003 with the forcing frequency (ω) of 2.707 Hz

4.4 Temperature profiles

The experimental results of thermocouple T9 temperature variations as a function of time for a swirl wave motion at non-dimensional frequency (ω/ω_{11}) of 1 and non-dimensional amplitude (A/R) of 0.0022, 0.0026, and 0.003 with the forcing frequency (ω) of 2.707 Hz are shown in Fig.6. When the A/R value increases, consequently does the temperature variation during oscillation, however the temperature variation after oscillation is quite small. Temperature changes of (A/R) of 0.0022, 0.0026, and 0.003 are higher when compared to experimental result without oscillation. Due to the swirl-breaking motion, the temperature of the liquid increases while the temperature of the vapour decreases during lateral sloshing. As the liquid (in the case of the asymmetric sloshing mode (1, 1)) flows up the hot wall of the upper half of the test rig, heat transfer from the wall owing to swirl and breaking motion of the liquid causes a portion of the increase in liquid temperature. Sloshing causes the temperature of thermocouples T7 to T12, which are located in the vapour zone, to quickly drops; nevertheless, after sloshing, the temperature abruptly increases. The temperature of thermocouples T1 to T6 lowers and increases as a result of lateral sloshing, which are located in the liquid zone. For Experiments 1 and 2, as the forcing amplitude increases, the wave motion gradually changes into a swirl and breaking motions, which has significant effects on thermocouple T1 to T12 temperature variations.

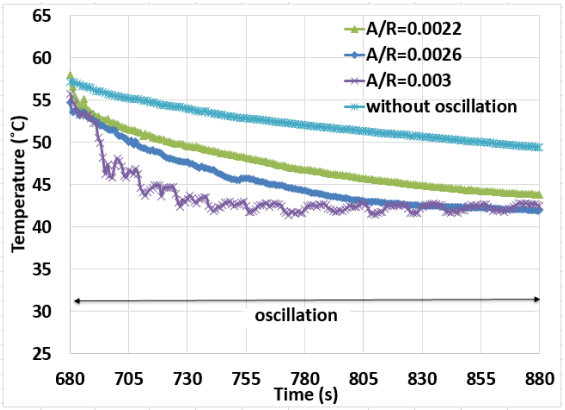

Fig.6. Temperature variations as a function of time (s) for swirl wave motion at non-dimensional frequency (ω/ω_{11}) of 1 and non-dimensional amplitude (A/R) having values 0.0022, 0.0026, and 0.003 with the forcing frequency (ω) of 2.707 Hz; corresponding temperature distributions of thermocouple T9 at vapour region

The temperature variations of the thermocouple at different heights, i.e., before heating, before vapour supply, end of vapour supply, and end of oscillation regions, have been measured for n-pentane under the conditions of stable wave and breaking wave (with swirl motion along the clockwise direction and for breaking/chaotic wave motion). In absence of oscillation, the pressure is found to decrease with time. In presence of oscillations for different amplitude ratios, the trend of pressure decrease is similar but the pressure itself is smaller than that in absence of oscillations. Due to vapour condensation at the liquid surface and on the test rig's top heated walls, the liquid depth marginally increases during vapour supply and oscillation regions. Condensation has a significant role in changing pressure and temperature values during lateral oscillation due to liquid movements (planner-breaking, breaking/chaotic-swirl, swirl-breaking, and swirl-planner).

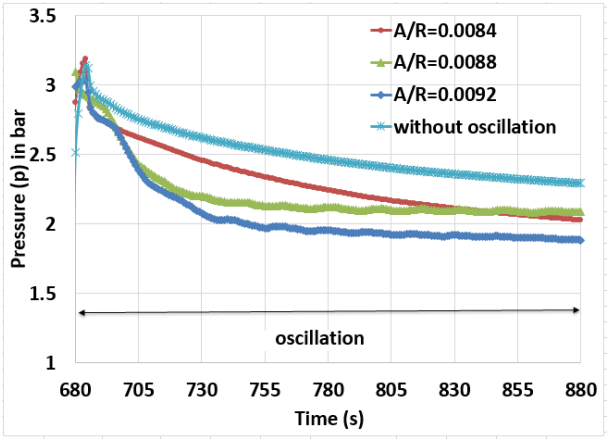

Fig.7. Pressure variations as a function of time (s) for breaking/chaotic wave regime (chaotic motion) with ω/ω_{11}=0.98 and A/R values of 0.0084, 0.0088, and 0.0092 respectively, with ω = 2.653 Hz

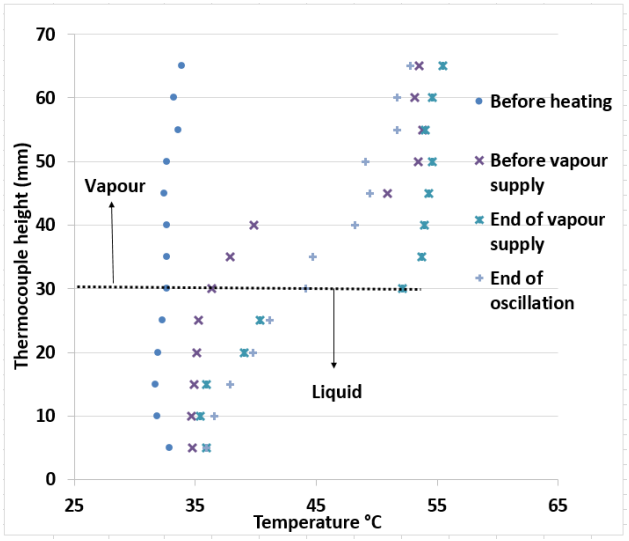

Fig.8. Temperature variations as a function of time (s) during before heating, before vapour supply, end of vapour supply, and end of oscillation; ω/ω_{11}=1 and the non-dimensional amplitude ratio A/R = 0.0018

As a result, the temperature gradient is strong near the liquid surface than it is elsewhere. According to the temperature profiles, the temperature in the vapour phase is almost uniform after ramping. With the exception of the interfacial zone, where a rapid temperature spike occurs over less than 0.5 cm, the temperature in the liquid region is uniform for the most part. After sloshing, the temperature in the vapour layer decreases and rises in the liquid layer, with the temperature gradient nearly reaching the entire liquid depth due to liquid movements, as shown in Figs. 3 and 6. Fig. 7 shows pressure variations with respect to time for breaking/chaotic wave regime at non-dimensional frequency (ω/ω_{11}) values of 0.98 and non-dimensional amplitude (A/R) values of 0.0084, 0.0088, and 0.0092, and with the forcing frequency of 2.653 Hz. The experimental 2 conditions are completely at breaking/chaotic wave regimes; as the amplitude increases, the wave motion changes from breaking or breaking to chaotic, as shown in Fig.4. The pressure drop increases during oscillation and decreases less after oscillation, as we have seen. Additionally, Fig. 7 amply demonstrates how the pressure drop values increase as the amplitude (A/R) ratio rises. The pressure drop occurs during oscillation and is larger when compared to the curve without oscillation. Also, the pressure and temperature change is less at the breaking/chaotic motion regime compared to swirl regime. Furthermore, pressure and temperature fluctuations are quite small as compared to experiment 1 conditions. The

temperature variations of the liquid and vapour section thermocouples for before heating, before vapour supply, end of vapour supply, and end of oscillation conditions are explained in Fig. 8. According to these experiments, the liquid movement (breaking/chaotic to swirl, swirl to planar motion) causes temperature changes to be larger in the liquid and vapour regions during sloshing. Following oscillation, the temperature readings of the liquid section thermocouples and the vapour section thermocouples both rise significantly due to swirl and breaking/chaotic motion. Additionally, experiments 1 and 2 make it clearly apparent that swirl and breaking/chaotic motions significantly influence changes in pressure and temperature. Furthermore, the results unambiguously demonstrate that, compared to the breaking/chaotic regime, the pressure and temperature variations are more in the swirl regime.

3. Conclusion

It is explained in this paper that large amplitude interfacial waves significantly boost heat and mass transfer at the liquid-vapour interface. According to the experimental investigations, the large pressure drop and temperature variation happens between 100 to 180 seconds during sloshing time. The rate of pressure drop is higher at the beginning of sloshing when temperature gradient is high and then it decreases. Accordingly, temperature drops in the vapour and increases in liquid due to condensation. Due to vapour condensation at the liquid surface and in the hot walls of the test rig, temperature increases during active pressurization. This condensation induces agitation and, as a result, temperature homogenization at both the liquid free surface and the vapour area. Temperature of bulk liquid increases by diffusion. During sloshing motion cold wall is exposed to the hot vapour causing enhanced condensation and with larger wave amplitude it is further enhanced. Thus the rate of pressure drop increases with increase in forcing amplitude. Near the natural frequency wave motion is swirl type with high amplitude and it increases with amplitude of forcing and so is the rate of pressure drop which is due to the exposure of larger cold wall to hot vapor. The drop is little less in chaotic regime as most of the condensation occurs on the free surface.

Acknowledgements

The first author would like to express his sincere gratitude for the fellowship sponsored by ANSYS during his Ph.D. research in the Department of Mechanical Engineering, Indian Institute of Technology Madras.

References

1) E.M. Moran, N.B. McNeils, M.T. Kudlac, M.S. Haberbusch, G.A. Satorino, Experimental results of hydrogen slosh in a 62 cubic foot (1750 liter) tank, in: 30th Joint Propulsion Conference, 1994, AIAA-94-3259.
2) T. Arndt, Sloshing of Cryogenic Liquids in a Cylindrical Tank under normal Gravity Conditions, first ed., Cuvillier Verlag Göttingen, Göttingen, 2012. p. 102.
3) S.P. Das and Hopfinger, E. J., Parametrically forced gravity waves in a circular cylinder and finite-time singularity." *Journal of Fluid Mechanics* 599 (2008): 205-228.
4) S.P. Das and E.J. Hopfinger, Mass transfer enhancement by capillary waves at a liquid–vapour interface, Int. J. Heat Mass Transfer 52 (5) (2009) 1400–1411.
5) E.J. Hopfinger and S.P. Das, Mass transfer enhancement by capillary waves at a liquid–vapour interface, Exp. Fluids 46 (4) (2009) 597–605.
6) C. Ludwig, M. E. Dreyer and E. J, Hopfinger, Pressure variations in a cryogenic liquid storage tank subjected to periodic excitations, International Journal of Heat and Mass Transfer 66, 223–234, 2013.
7) J. Lacapere, Results of the sloshing tests with LOX, AIR LIQUID Report No. RTRE-22R22-0501-AIRL-01, 2005.